Carbonili omoleptici

Table 21.5 Formulas and electron count for some 3d-series carbonyls

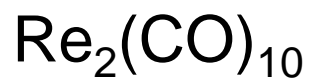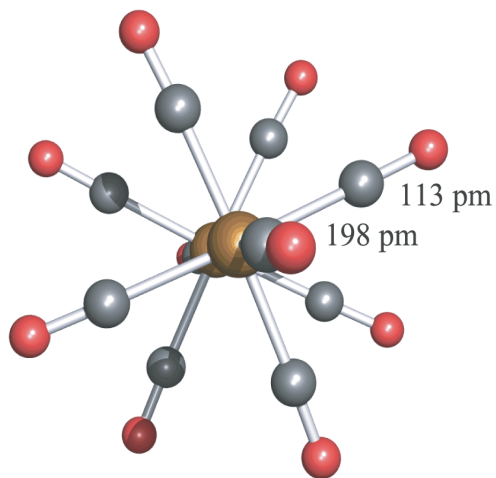| Group	Formula	Valence electrons		Structure
6	$Cr(CO)_6$	Cr	6	
		6(CO)	12	
			18	
7	$Mn_2(CO)_{10}$	Mn	7	
		5(CO)	10	
		M—M	1	
			18	
8	$Fe(CO)_5$	Fe	8	
		5(CO)	10	
			18	
9	$Co_2(CO)_8$	Co	9	
		4(CO)	8	
		M—M	1	
			18	
10	$Ni(CO)_4$	Ni	10	
		4(CO)	8	
			18	

Re$_2$(CO)$_{10}$

14 + 20 +2 = 36e$^-$

Fe$_2$(CO)$_9$

16 + 18 +2 = 36e$^-$

Co$_2$(CO)$_8$

18 + 16 +2 = 36e$^-$

Reazione diretta

$$Ni(s) + 4CO(g) \xrightarrow{50\ °C,\ 1\ atm\ CO} Ni(CO)_4(g)$$

$$Fe(s) + 5CO(g) \xrightarrow{200\ °C,\ 200\ atm} Fe(CO)_5(l)$$

$$2Co(s) + 8CO(g) \xrightarrow{150\ °C,\ 35\ atm} Co_2(CO)_8(s)$$

Thermocouple

High-pressure gas supply

Metal thermocouple well

Glass container

Stainless steel pressure vessel
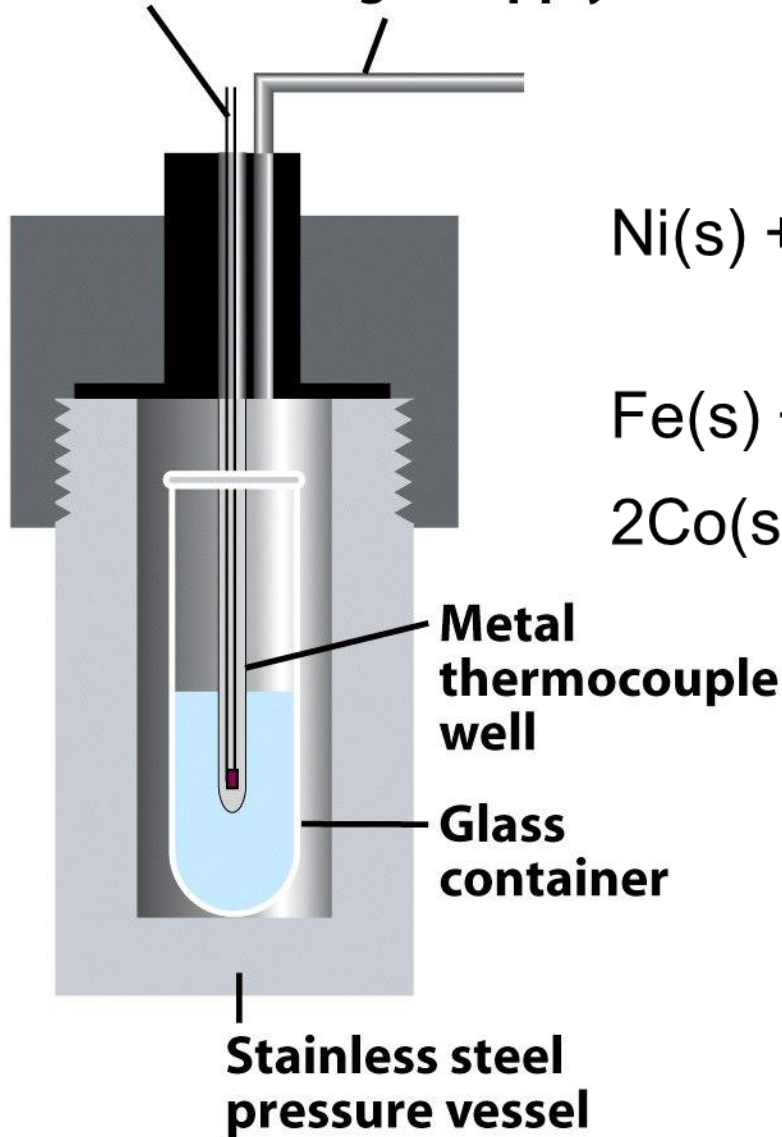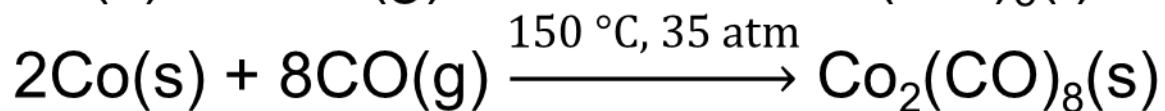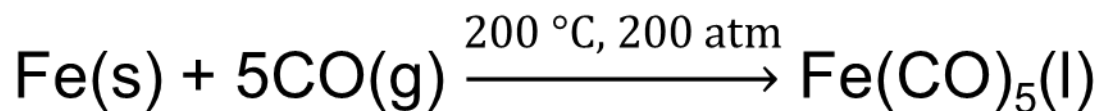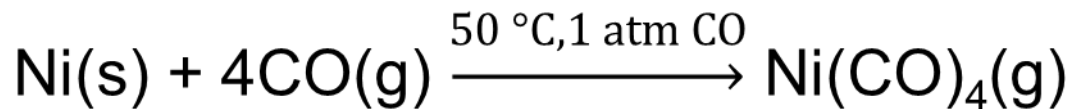
L.—Action of Carbon Monoxide on Nickel.

By Ludwig Mond, Dr. Carl Langer, and Dr. Friedrich Quincke.

When carbon monoxide is passed over finely-divided metallic nickel at a temperature between 350° and 450°, carbon dioxide is formed, and a black, amorphous powder is obtained consisting of nickel and carbon. The composition of this powder varies very widely with the temperature employed, and still more according to the time the operation has been carried on. A small quantity of nickel can decompose a very large amount of carbon monoxide. At the commencement, a fast current of carbon monoxide is completely changed into carbon dioxide by a comparatively small quantity of nickel. By-and-by, the change becomes less complete, but the gas may be passed for several weeks before carbon dioxide ceases to be formed.

We have in this way obtained a product containing as much as 85 per cent. carbon and 15 per cent. nickel. By treating this product with acids, a certain portion of the nickel goes into solution; but we have not been able to extract the nickel completely, the minimum quantity remaining after treatment with concentrated sulphuric acid being 5·59 per cent.; by treatment with dilute hydrochloric acid, 9·30 per cent.[*]

In order to determine the nickel in this substance, we have heated it with concentrated sulphuric acid to about 200°, and then added nitrate of potash in small portions to oxidise the carbon. This was the only way by which we could obtain a perfectly clear solution, and

[*] Gautier and Hallopeau (*Compt. rend.*, **108**, 1889, 1111) obtained a similar product containing 20·05 per cent. of nickel and 79·95 per cent. carbon, by acting with

had been increased, thus proving that one volume of our compound gives 4 volumes of carbon monoxide. We give the result of several analyses, which lead to the formula $Ni(CO)_4$.

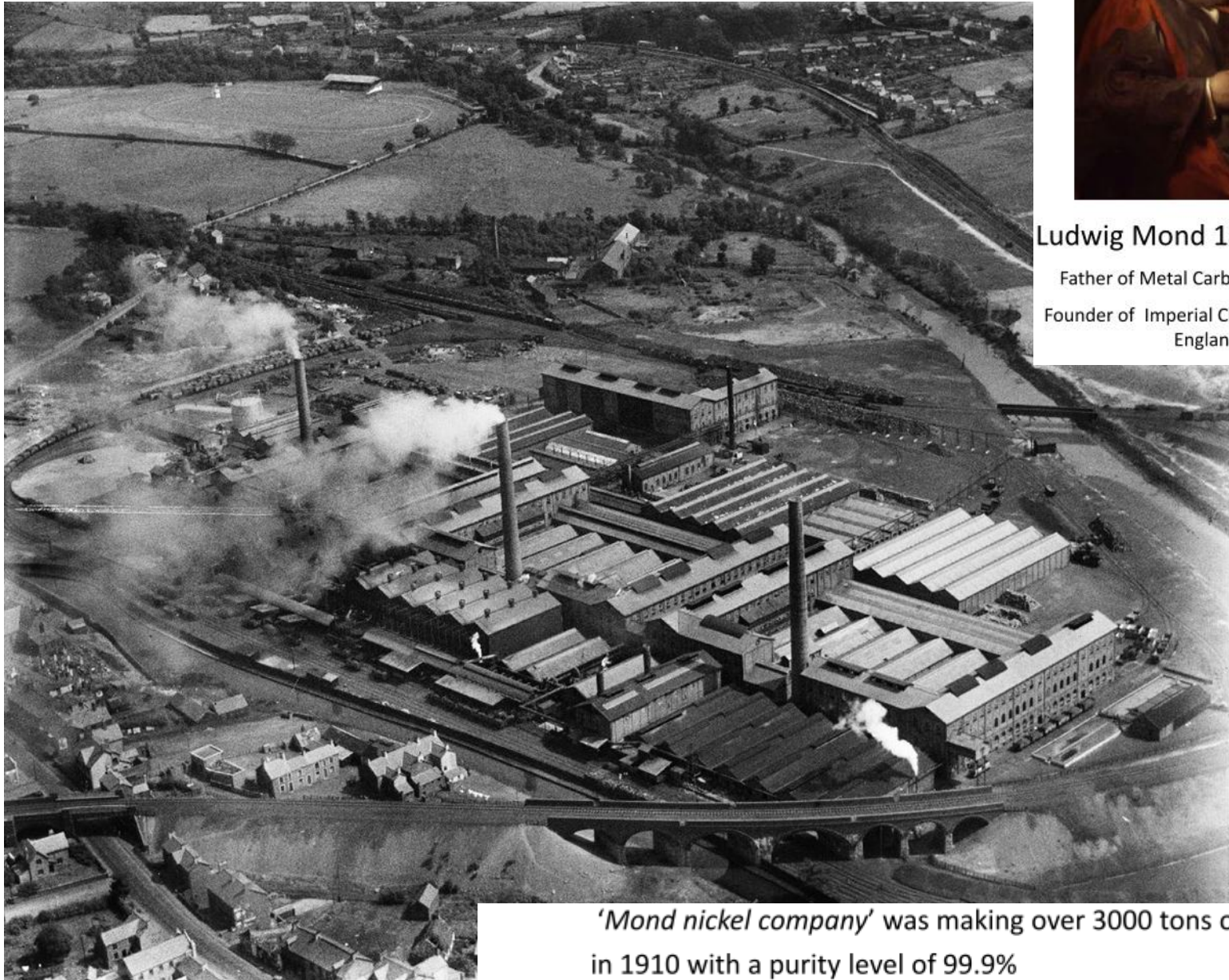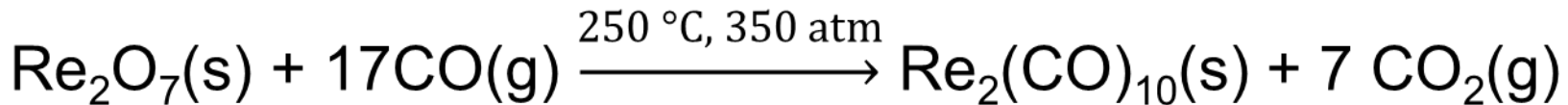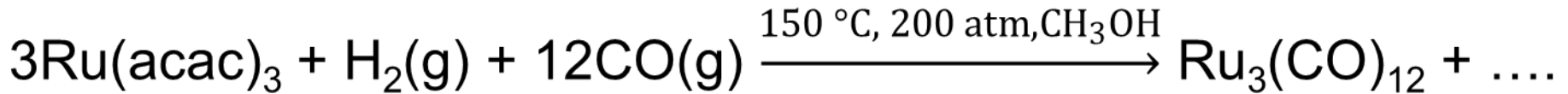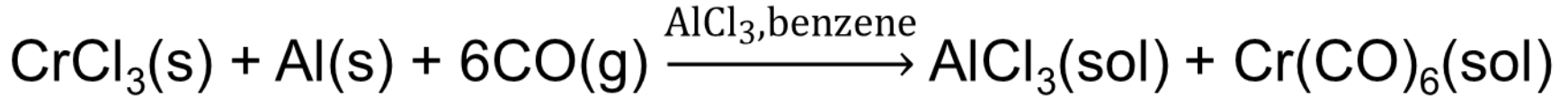# Mond Nickel Works, Clydach (Wales)
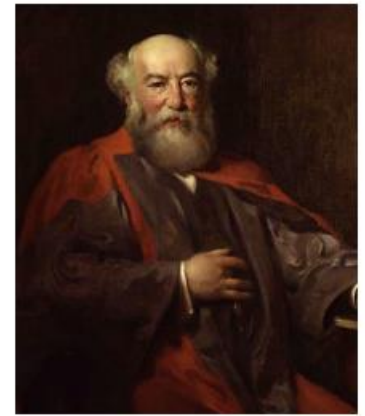
Ludwig Mond 1839-1909

Father of Metal Carbonyl Chemistry

Founder of Imperial Chemical Industry, England
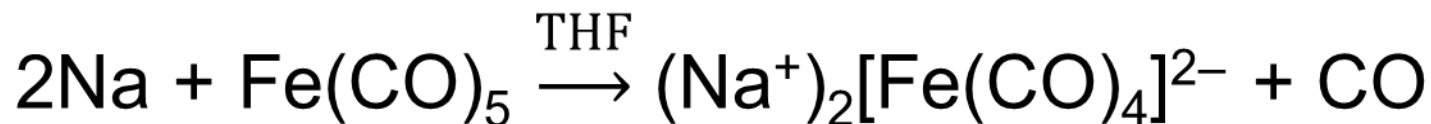
'*Mond nickel company*' was making over 3000 tons of nickel in 1910 with a purity level of 99.9%

Carbonilazione riduttiva

$$CrCl_3(s) + Al(s) + 6CO(g) \xrightarrow{\text{AlCl}_3,\text{benzene}} AlCl_3(sol) + Cr(CO)_6(sol)$$

$$3Ru(acac)_3 + H_2(g) + 12CO(g) \xrightarrow{150\,°C,\ 200\ \text{atm},\text{CH}_3\text{OH}} Ru_3(CO)_{12} + \ldots.$$

$$Re_2O_7(s) + 17CO(g) \xrightarrow{250\,°C,\ 350\ \text{atm}} Re_2(CO)_{10}(s) + 7\ CO_2(g)$$

Group number	5	6	7	8	9	10
First row metals	$V(CO)_6$ Dark blue solid; paramagnetic; dec. 343 K	$Cr(CO)_6$ White solid; sublimes *in vacuo*; dec. 403 K	$Mn_2(CO)_{10}$ Yellow solid; mp 427 K	$Fe(CO)_5$ Yellow liquid; mp 253 K; bp 376 K $Fe_2(CO)_9$ Golden crystals; mp 373 K (dec.) $Fe_3(CO)_{12}$ Dark green solid; dec. 413 K	$Co_2(CO)_8$ Air-sensitive, orange-red solid; mp 324 K $Co_4(CO)_{12}$ Air-sensitive, black solid $Co_6(CO)_{16}$ Black solid; slowly dec. in air	$Ni(CO)_4$ Colourless, volatile liquid; highly toxic vapour; bp 316 K
Second row metals		$Mo(CO)_6$ White solid; sublimes *in vacuo*	$Tc_2(CO)_{10}$ White solid; slowly dec. in air; mp 433 K	$Ru(CO)_5$ Colourless liquid; mp 251 K; dec. in air at 298 K to $Ru_3(CO)_{12} + CO$ $Ru_3(CO)_{12}$ Orange solid; mp 427 K; sublimes *in vacuo*	$Rh_4(CO)_{12}$ Red solid; >403 K dec. to $Rh_6(CO)_{16}$ $Rh_6(CO)_{16}$ Black solid; dec. >573 K	
Third row metals		$W(CO)_6$ White solid; sublimes *in vacuo*	$Re_2(CO)_{10}$ White solid; mp 450 K	$Os(CO)_5$ Yellow liquid; mp 275 K $Os_3(CO)_{12}$ Yellow solid;	$Ir_4(CO)_{12}$ Slightly air-sensitive yellow solid; mp 443 K $Ir_6(CO)_{16}$ Red solid	

Riduzione dei metallocarbonili a metallocarbonilati

$$2Na + Fe(CO)_5 \xrightarrow{THF} (Na^+)_2[Fe(CO)_4]^{2-} + CO$$

ν_{CO} 1730 cm^{-1}

117 pm

175 pm

$[Fe(CO)_4]^{2-}$
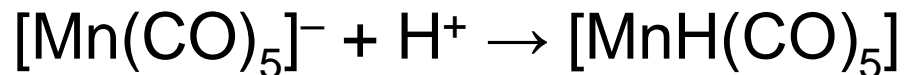
$$2Na + (OC)_5Mn-Mn(CO)_5 \xrightarrow{THF} 2Na[Mn(CO)_5]$$
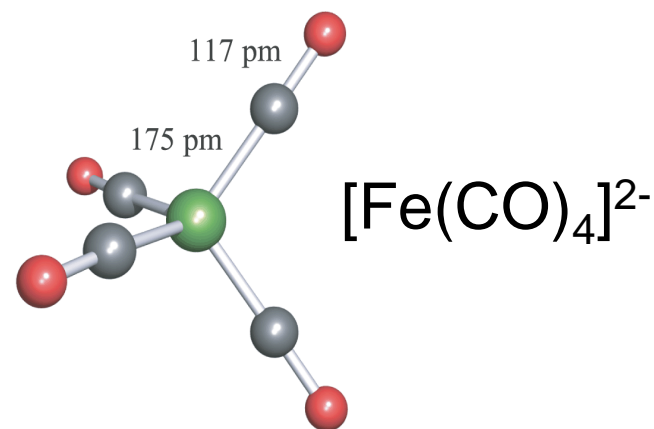
Table 21.6 Acidity constants of *d*-metal hydrides in acetonitrile at 25°C

Hydride	pK_a
$[CoH(CO)_4]$	8.3
$[CoH(CO)_3P(OPh)_3]$	11.3
$[Fe(H)_2(CO)_4]$	11.4
$[CrH(Cp)(CO)_3]$	13.3
$[MoH(Cp)(CO)_3]$	13.9
$[MnH(CO)_5]$	15.1
$[CoH(CO)_3PPh_3]$	15.4
$[WH(Cp)(CO)_3]$	16.1
$[MoH(Cp*)(CO)_3]$	17.1
$[Ru(H)_2(CO)_4]$	18.7
$[FeH(Cp)(CO)_2]$	19.4
$[RuH(Cp)(CO)_2]$	20.2
$[Os(H)_2(CO)_4]$	20.8
$[ReH(CO)_5]$	21.1
$[FeH(Cp*)(CO)_2]$	26.3
$[WH(Cp)(CO)_2PMe_3]$	26.6

Protonazione di metallocarbonilati

$$[Mn(CO)_5]^- + H^+ \rightarrow [MnH(CO)_5]$$

Basicità dei metallocarbonilati:
Attacco nucleofilo

$[Mn(CO)_5]^- + CH_3I \rightarrow [Mn(CH_3)(CO)_5] + I^-$

$[Co(CO)_4]^- + CH_3COI \rightarrow [Co(COCH_3)(CO)_4] + I^-$

$[Mn(CO)_5]^- + [ReBr(CO)_5] \rightarrow [(OC)_5Mn-Re(CO)_5] + Br^-$
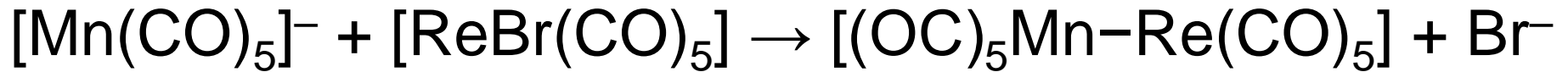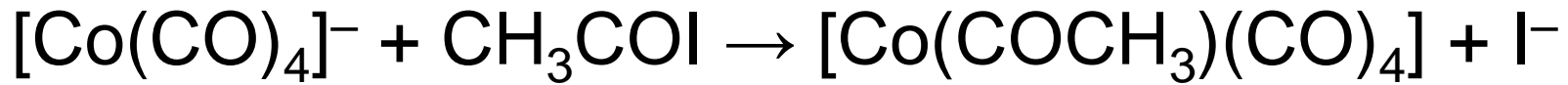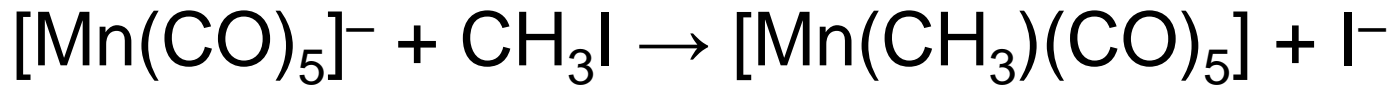
Ossidazione (rottura ossidativa) di un legame M−M in metallo-carbonili

$$[(OC)_5Mn^{(0)}-Mn^{(0)}(CO)_5] + Br_2 \rightarrow 2[Mn^{(+1)}Br(CO)_5]$$
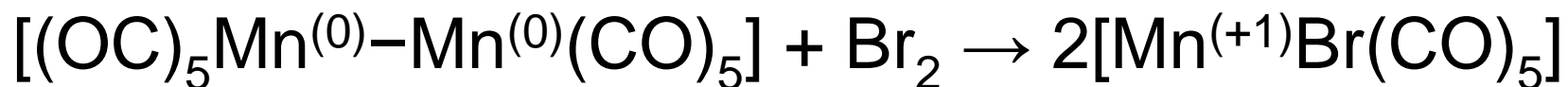
Attacchi nucleofili ed elettrofili a carbonili

Metallo elettron-povero: attacco nucleofilo su C

$$Li(CH_3) + [Mo(CO)_6] \rightarrow Li[Mo(COCH_3)(CO)_5]$$
$$[(OC)_nM(CO)] + OH^- \rightarrow [(OC)_nM(COOH)]^-$$
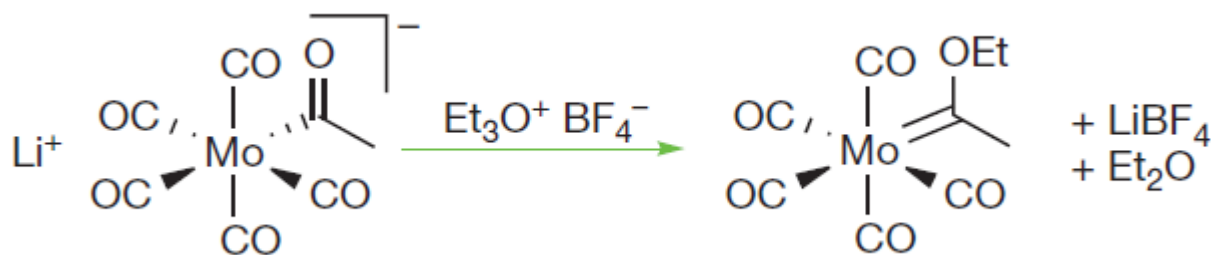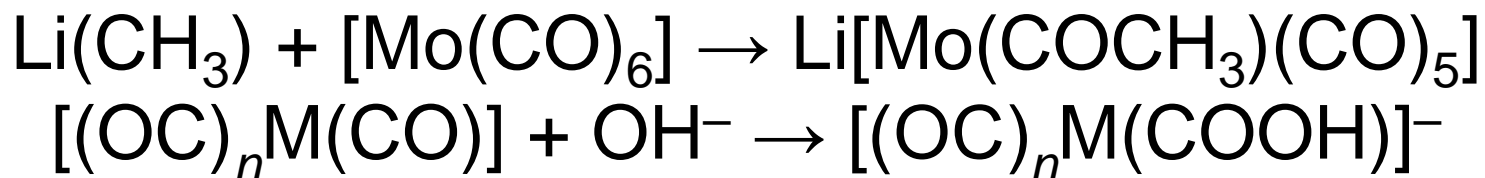
Metallo elettron-ricco: attacco elettrofilo su O
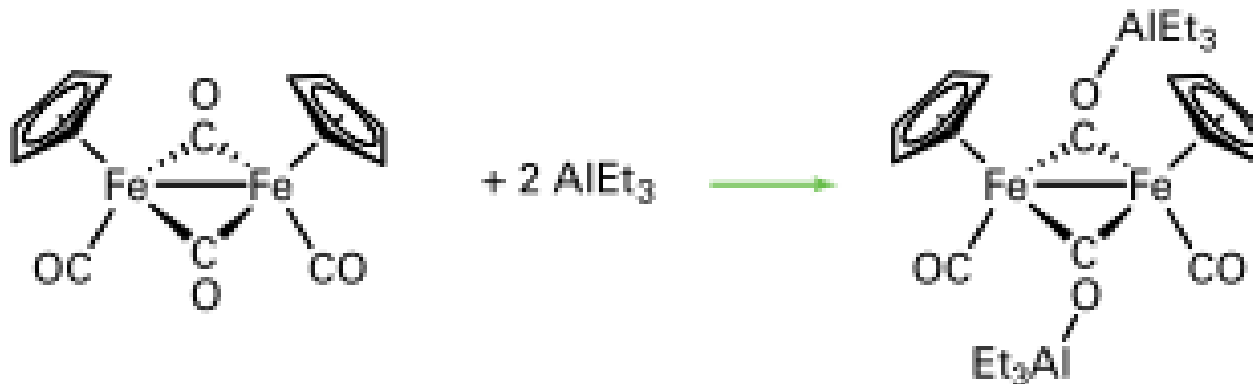
Table 21.7 Relation between the structure of a carbonyl complex and the number of CO stretching bands in its IR spectrum

Complex	Isomer	Structure	Point group	Number of bands*	Complex	Isomer	Structure	Point group	Number of bands*
$M(CO)_6$		octahedral	O_h	1	$M(CO)_5$		trigonal bipyramidal	D_{3h}	2
$M(CO)_5L$		octahedral	C_{4v}	3[†]	$M(CO)_5$	ax	trigonal bipyramidal	C_{3v}	3[§]
$M(CO)_4L_2$	trans	octahedral	D_{4h}	1	$M(CO)_4L$	eq	trigonal bipyramidal	C_{2v}	4
$M(CO)_4L_2$	cis	octahedral	C_{2v}	4[‡]	$M(CO)_3L_2$	trans	trigonal bipyramidal	D_{3h}	1
$M(CO)_3L_3$	mer	octahedral	C_{2v}	3[‡]	$M(CO)_3L_2$	cis	trigonal bipyramidal	C_s	3
$M(CO)_3L_3$	fac	octahedral	C_{3v}	2	$M(CO)_4$		tetrahedral	T_d	1

* The number of IR bands expected in the CO stretching region is based on formal selection rules, and in some cases fewer bands are observed, as explained below.
† If the fourfold array of CO ligands lies in the same plane as the metal atom, two bands will be observed.
‡ If the trans CO ligands are nearly collinear, one fewer band will be observed.
§ If the threefold array of CO ligands is nearly planar, only two bands will be observed.

Cluster carbonilico

$[Co_4(CO)_{12}]$

(d)

Co$_2$(CO)$_8$

(e)

Fe$_3$(CO)$_{12}$

(f)

Os$_3$(CO)$_{12}$
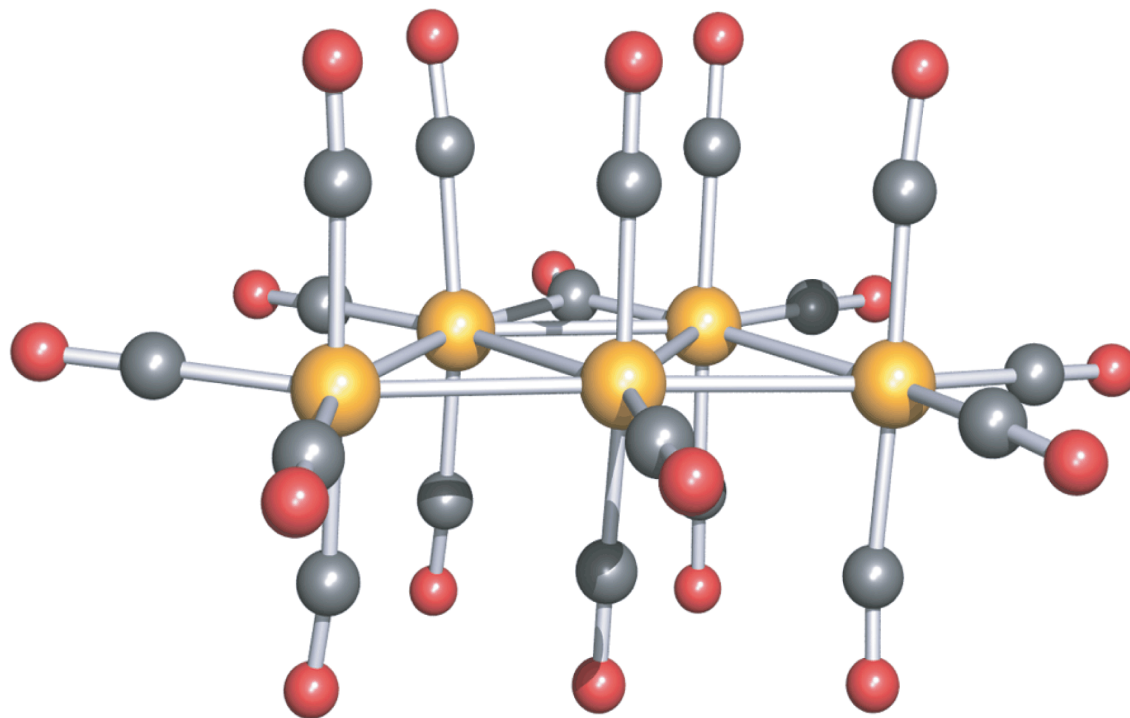
(a) $Rh_4(CO)_{12}$

(b) $Ir_4(CO)_{12}$

(c) $Ir_6(CO)_{16}$ rosso

(d) $Ir_6(CO)_{16}$ nero

$Os_5(CO)_{18}$
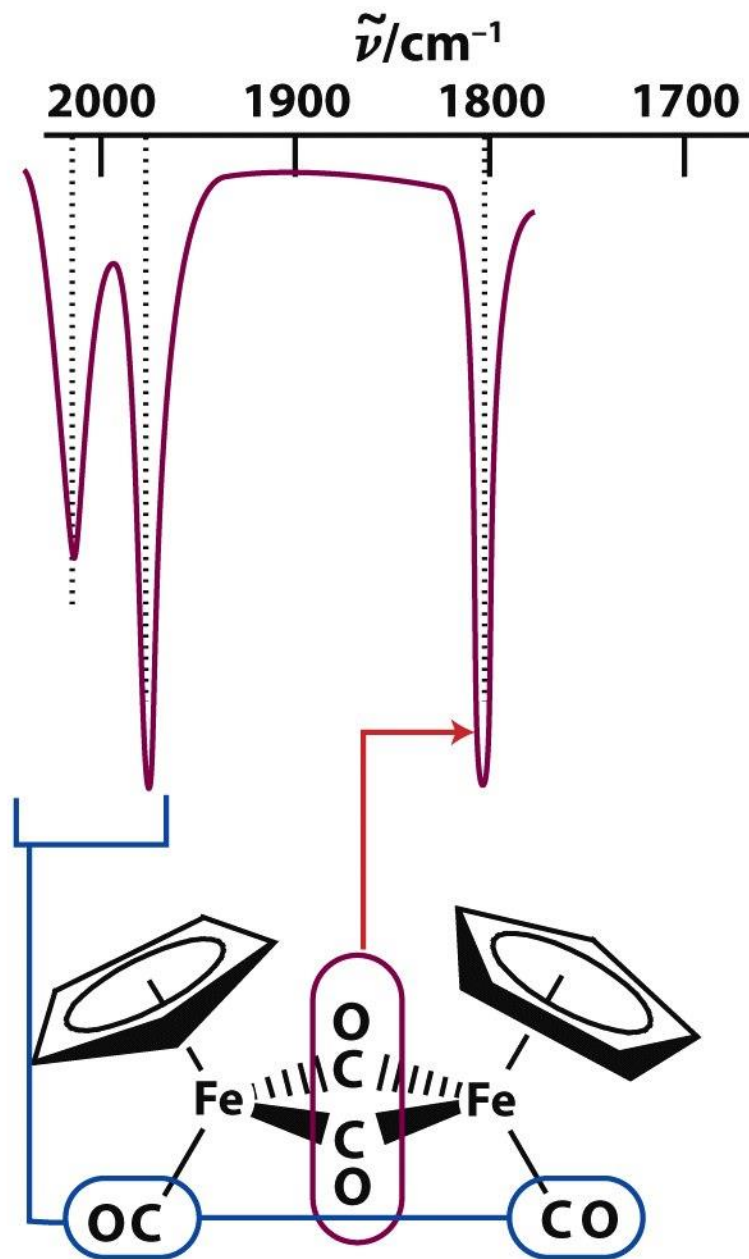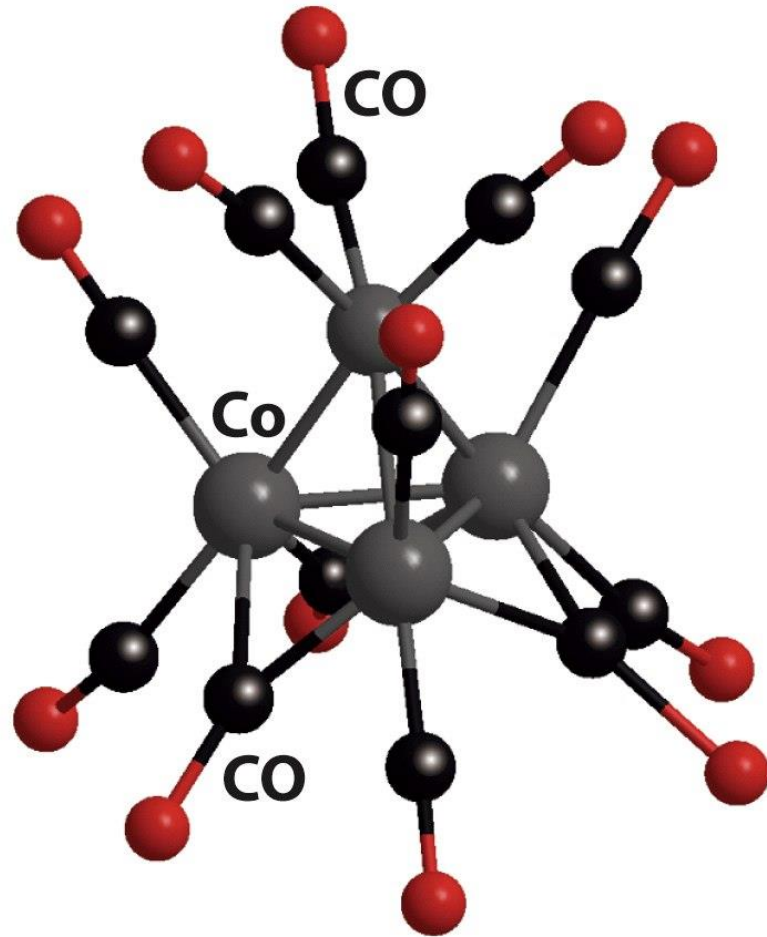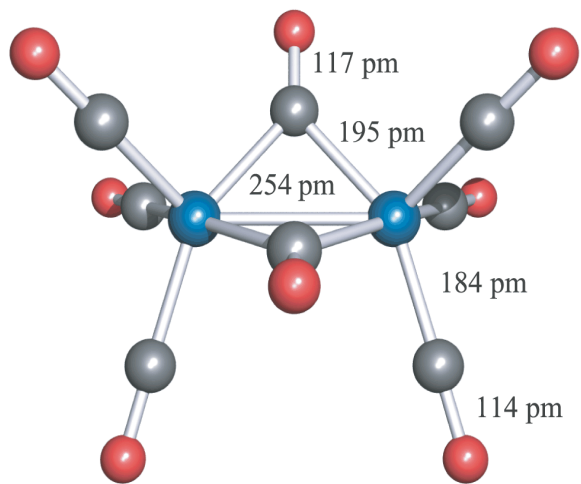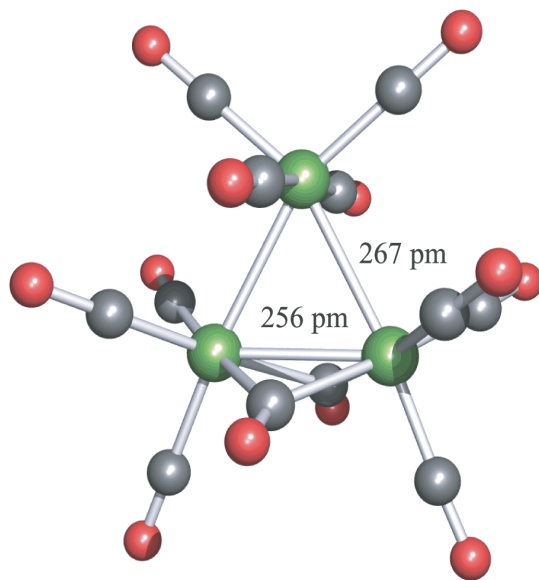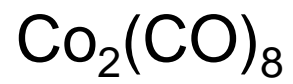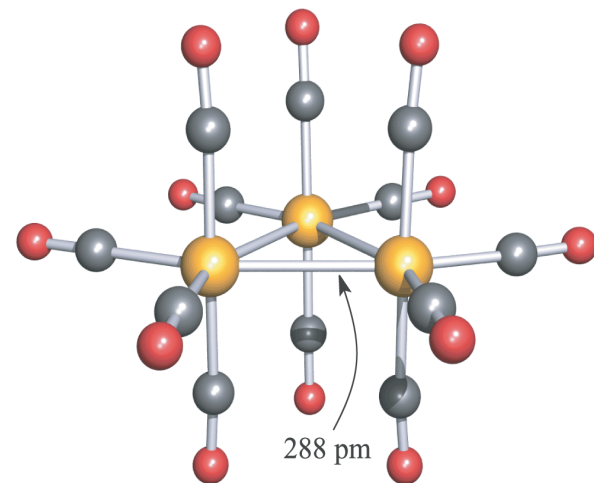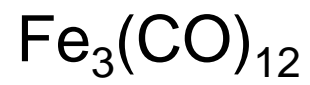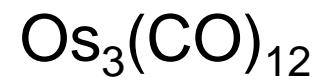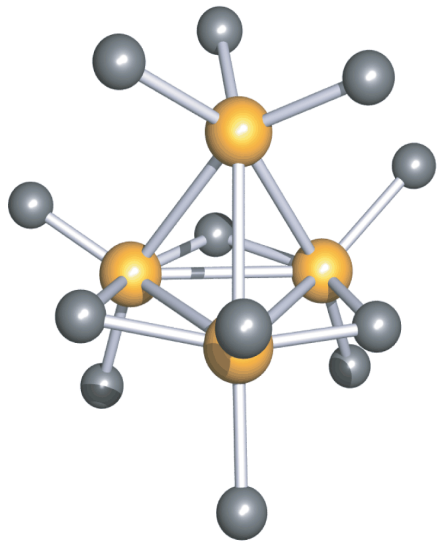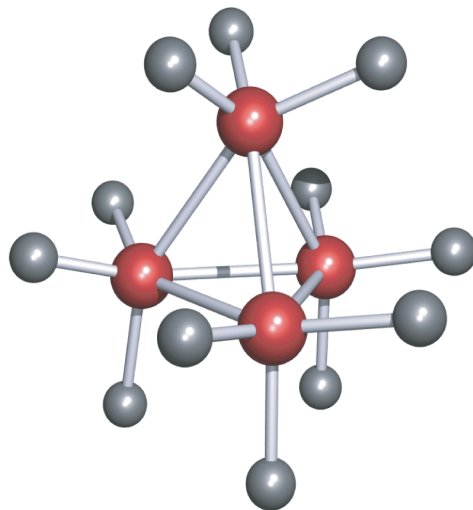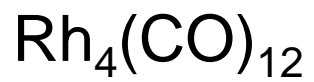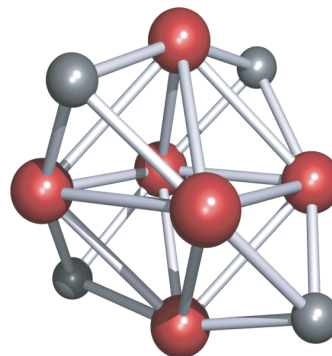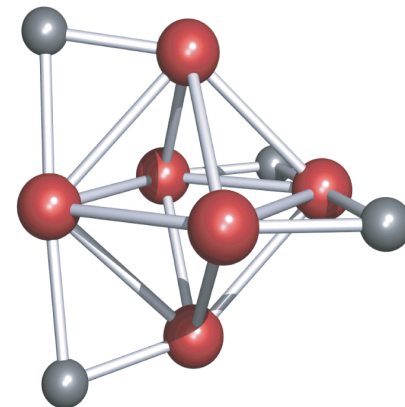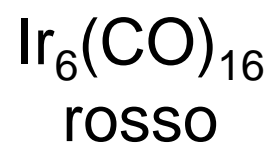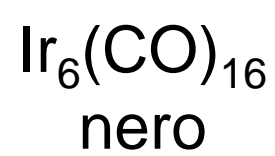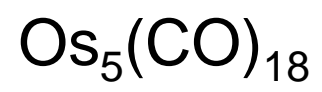
Ferrocene e Metalloceni

Fast rotation
($\Delta G^* = 4$ kJ·mol^{-1})

Fe   Fe

Eclipsed D_{5h} conformation
observed in solution by XAFS
at very low temperatures[353]

Staggered D_{5d} conformation
often observed in crystal structures
including for decamethylferrocene
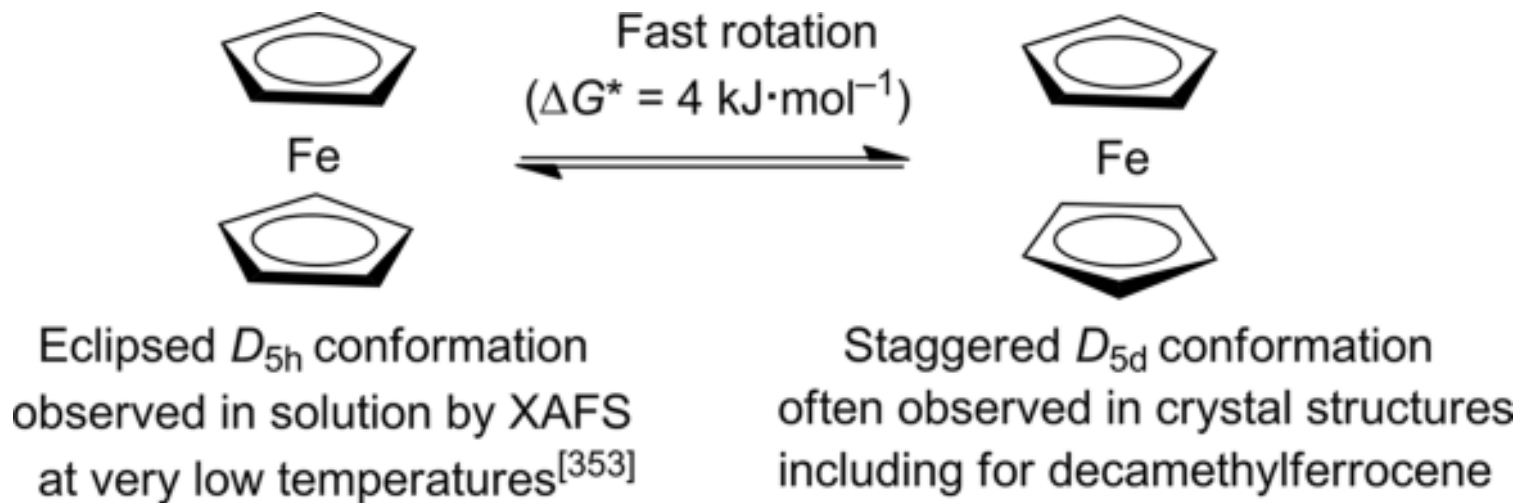
- G. Wilkinson, M. Rosenblum, M. C. Whiting, R. B. Woodward, *J. Am. Chem. Soc.* **1952**, *74*, 2125–2126.

- E. O. Fischer, W. Pfab, *Z. Naturforsch. B* **1952**, *7*, 377–379.

Nel 2017 si contavano più di 18000 pubblicazioni sui ferroceni

$$2Na + 2C_5H_6 \xrightarrow{\text{THF}} 2Na[C_5H_5] + H_2$$

$$2KOH + 2C_5H_6 + FeCl_2 \xrightarrow{\text{DMSO}} Fe(C_5H_5)_2 + 2H_2O + 2KCl$$
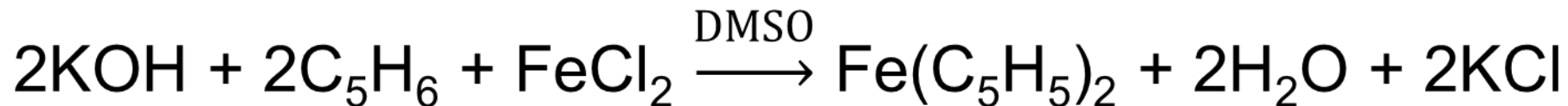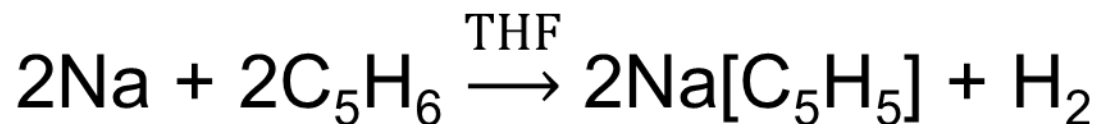
- Stabile fino a 400 ºC (fonde a 172 ºC)
- Stabile all'aria e solubile in molti solventi organici
- Reattività di un super-elettrofilo aromatico
- Ossidazione reversibile a +0.4 V vs SCE

CH$_3$COCl + AlCl$_3$
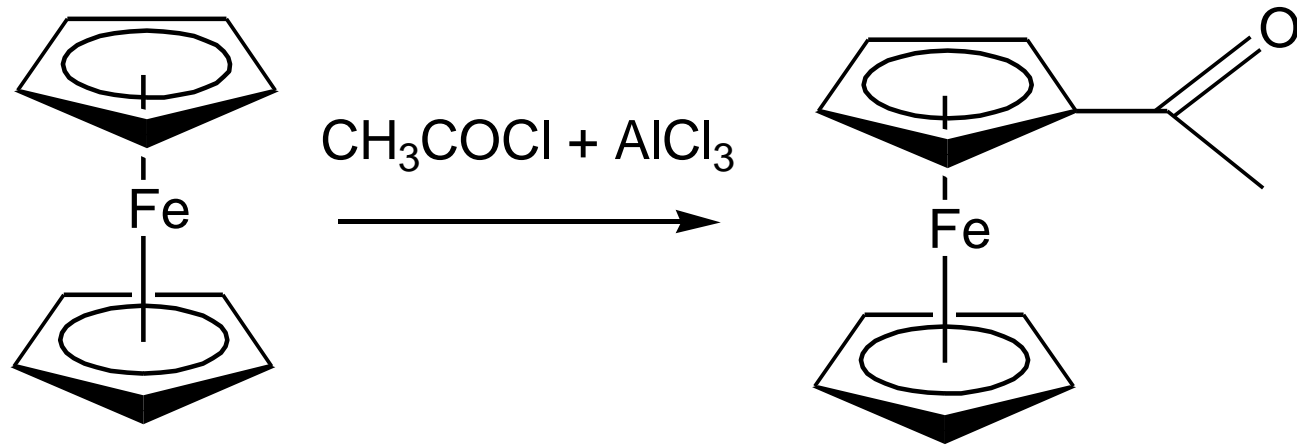
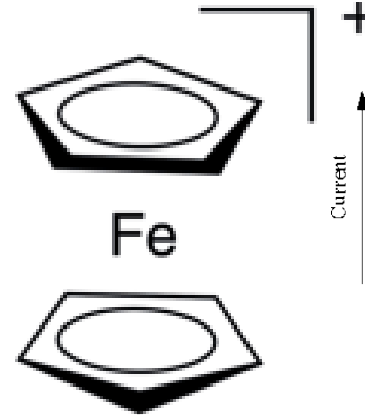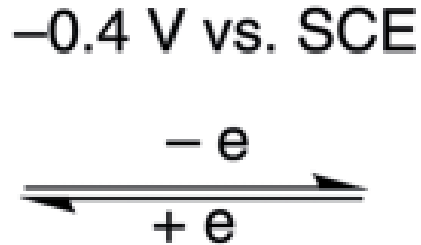acilazione di Friedel – Crafts

BuLi

+ BuH

RC(O)Cl, AlCl$_3$

Conc. H$_2$SO$_4$

$(\eta^5\text{-Cp})_2$Fe

Ph$_2$PCl, AlCl$_3$

^{n}BuLi,
Me$_2$NCH$_2$CH$_2$NMe$_2$

Ph$_2$PCl

Ph$_2$PCl

−0.4 V vs. SCE

$-e$ / $+e$

E_{pc}

$E_{1/2} = 1/2(E_{pc} + E_{pa})$

i_{pc}

Current

i_{pa}

E_{pa}

Increasing Positive Potential
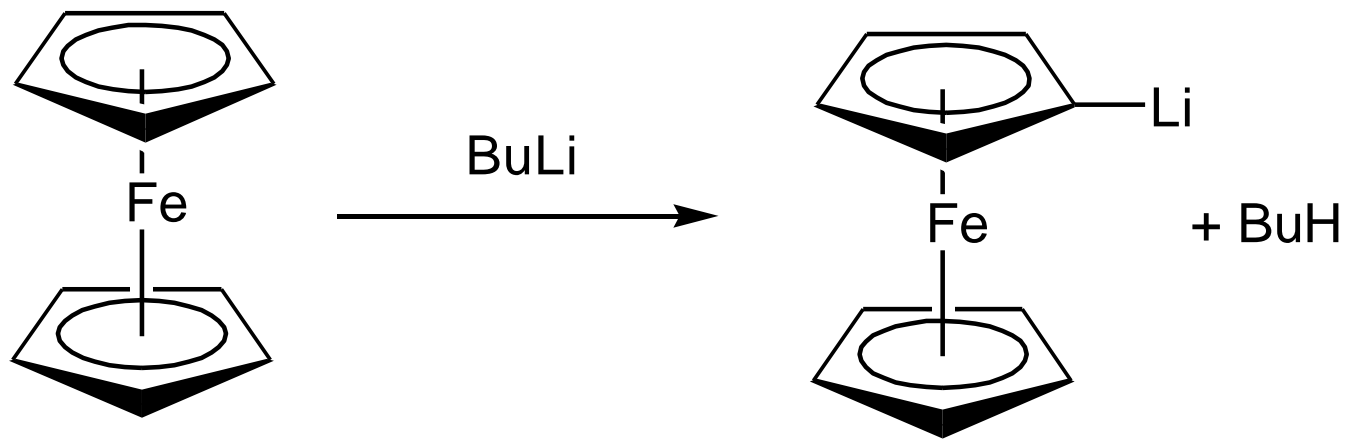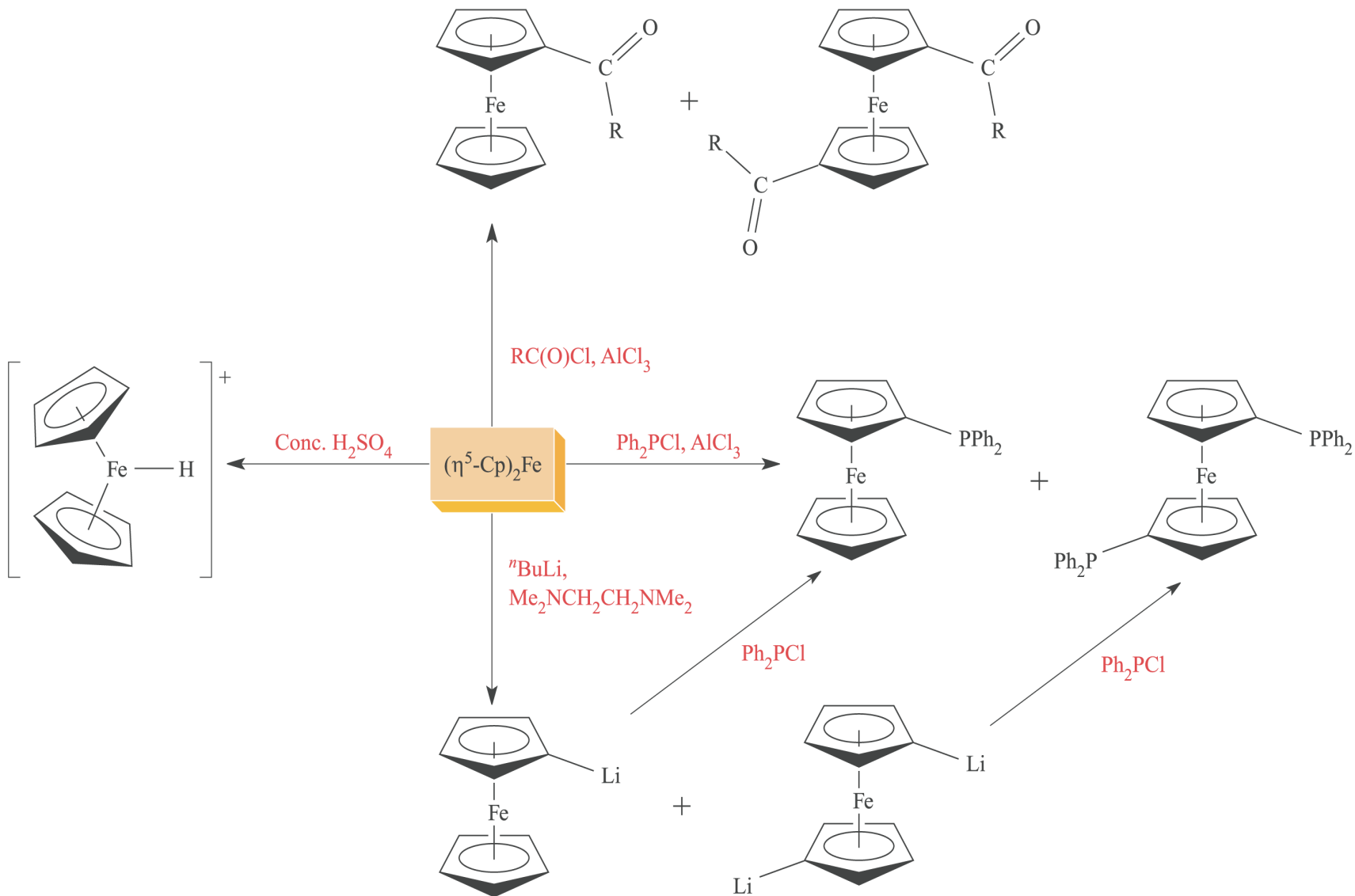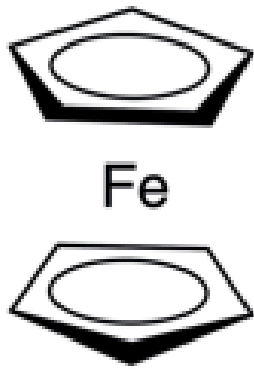
Ferrocene, orange
d^6, Fe^{II}, 18e
Functionalization with
non-oxidizing electrophiles

Ferricinium, deep-blue
d^5, Fe^{III}, 17e
Isolable as BF_4^- or PF_6^- salt, etc.
Sensive to O_2 and nucleophiles
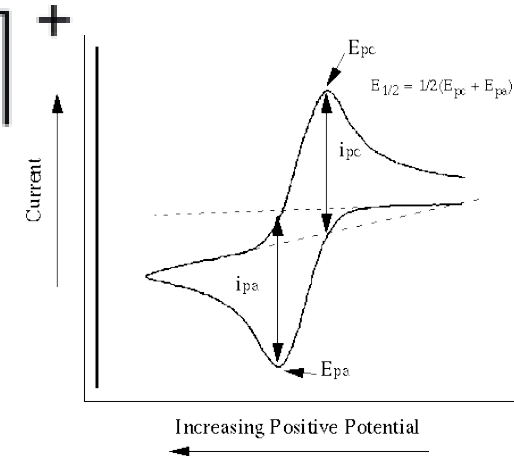
L'ossidazione è perfettamente reversibile, tanto che il ferrocene è usato come standard in voltammetria ciclica. Di conseguenza il ferricinio (17e⁻) deve essere piuttosto stabile.

3π

2π

1π

$d_{x^2-y^2}$ d_{xy} δ

d_{yz} d_{zx} π

d_{z^2} σ
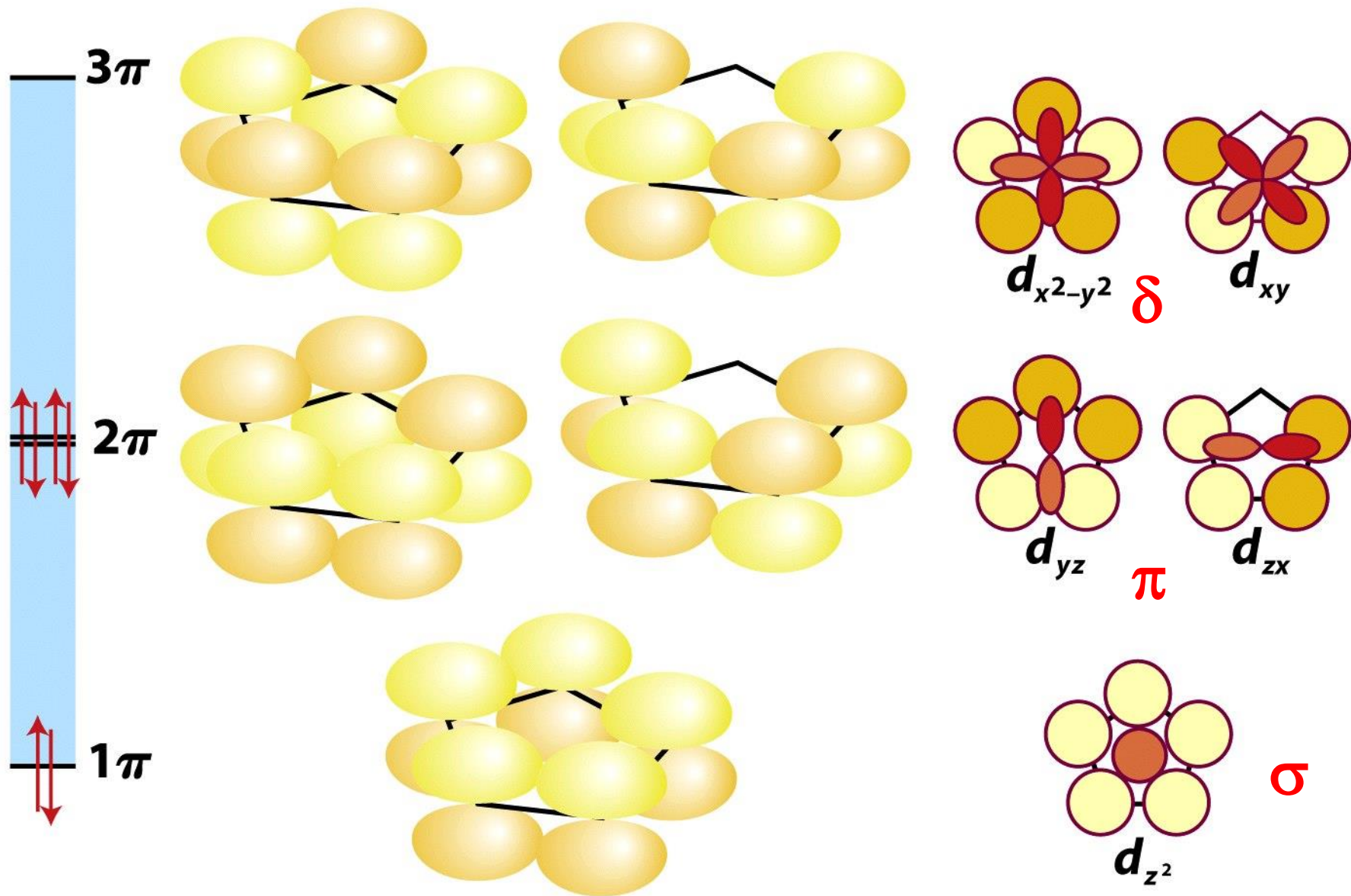
$(C_5H_5)_2{}^{2\text{-}}$ (D_{5h})

Ferrocene (D_{5h})

Fe^{2+}

e_1'

a_2''

a_1'

$5e_2'$

$4e_2'$

e_2''

e_2'

LUMO

$5e_1''$ (xz, yz)

retrodonazione δ

HOMO

$4e_2'$ ($x^2 - y^2, xy$)

$8a_1'$ (z^2)

e_1''

e_1'

$6e_1'$

$4e_1''$

donazione π

a_2''

a_1'

$6a_2''$

$7a_1'$

donazione σ

e_1'

a_2''

a_1'

4p

4s

xz, yz

e_1''

xy
x^2-y^2

e_2'

a_1'

3d
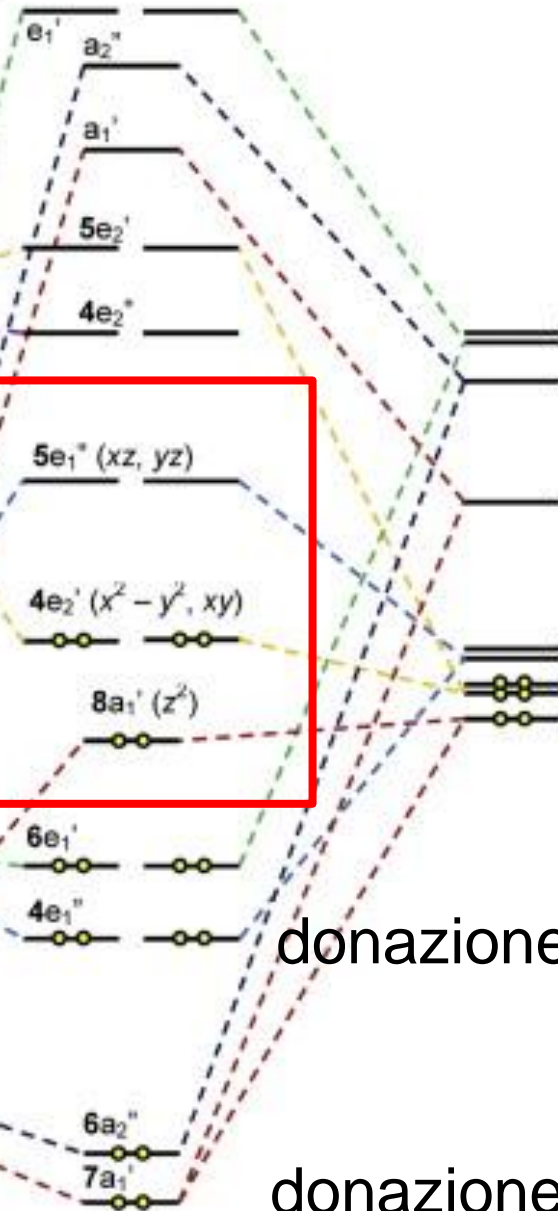
Table 21.8 Electronic configuration and M—C bond length in $[M(\eta^5\text{-Cp})_2]$ complexes

Complex	Valence electrons	Electron configuration	M—C bond length/pm
$[V(\eta^5\text{-Cp})_2]$	15	$e_2'^2 a_1'^1$	228
$[Cr(\eta^5\text{-Cp})_2]$	16	$e_2'^3 a_1'^1$	217
$[Mn(\eta^5\text{-Me-C}_5\text{H}_4)_2]^*$	17	$e_2'^3 a_1'^2$	211
$[Fe(\eta^5\text{-Cp})_2]$	18	$e_2'^4 a_1'^2$	206
$[Co(\eta^5\text{-Cp})_2]$	19	$e_2'^4 e_1''^1 a_1'^2$	212
$[Ni(\eta^5\text{-Cp})_2]$	20	$e_2'^4 e_1''^2 a_1'^2$	220

*Data are quoted for this complex because $[Mn(\eta^5\text{-Cp})_2]$ has a high-spin configuration and hence an anomalously long M—C bond (238 pm).

Bent sandwich

C_6H_6

Cr

CO
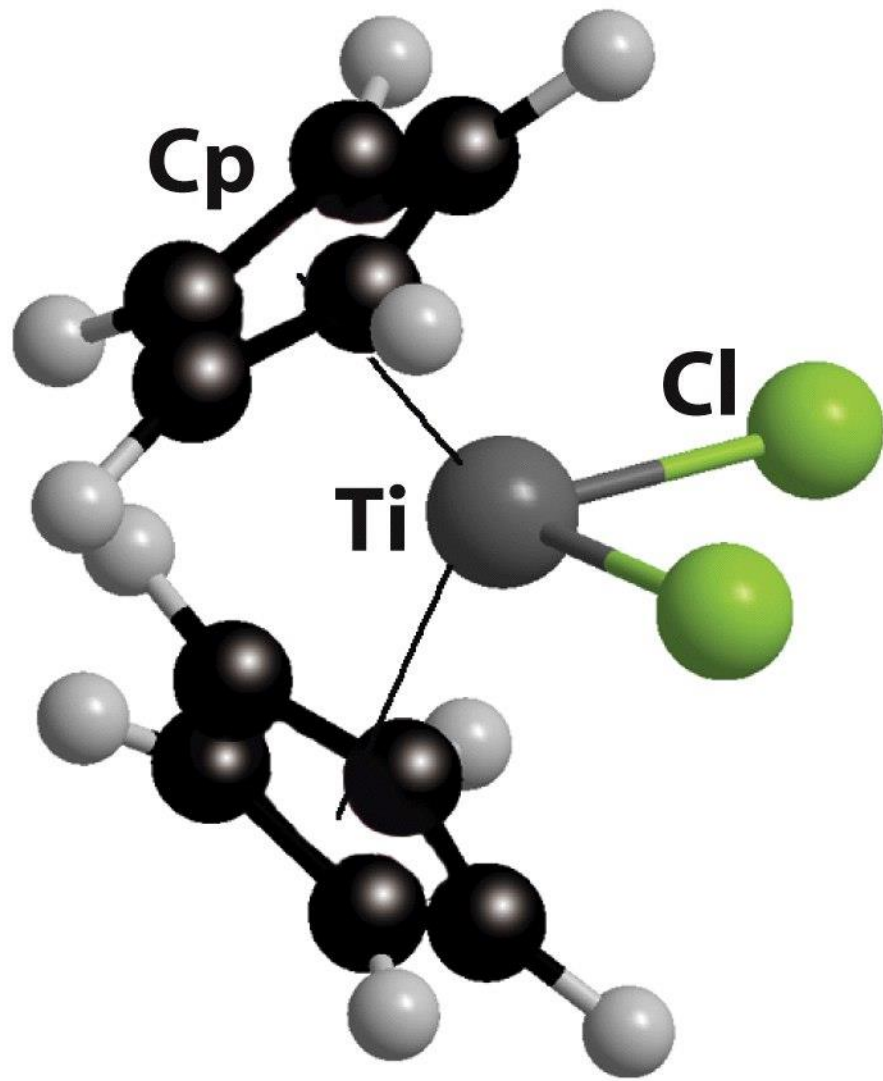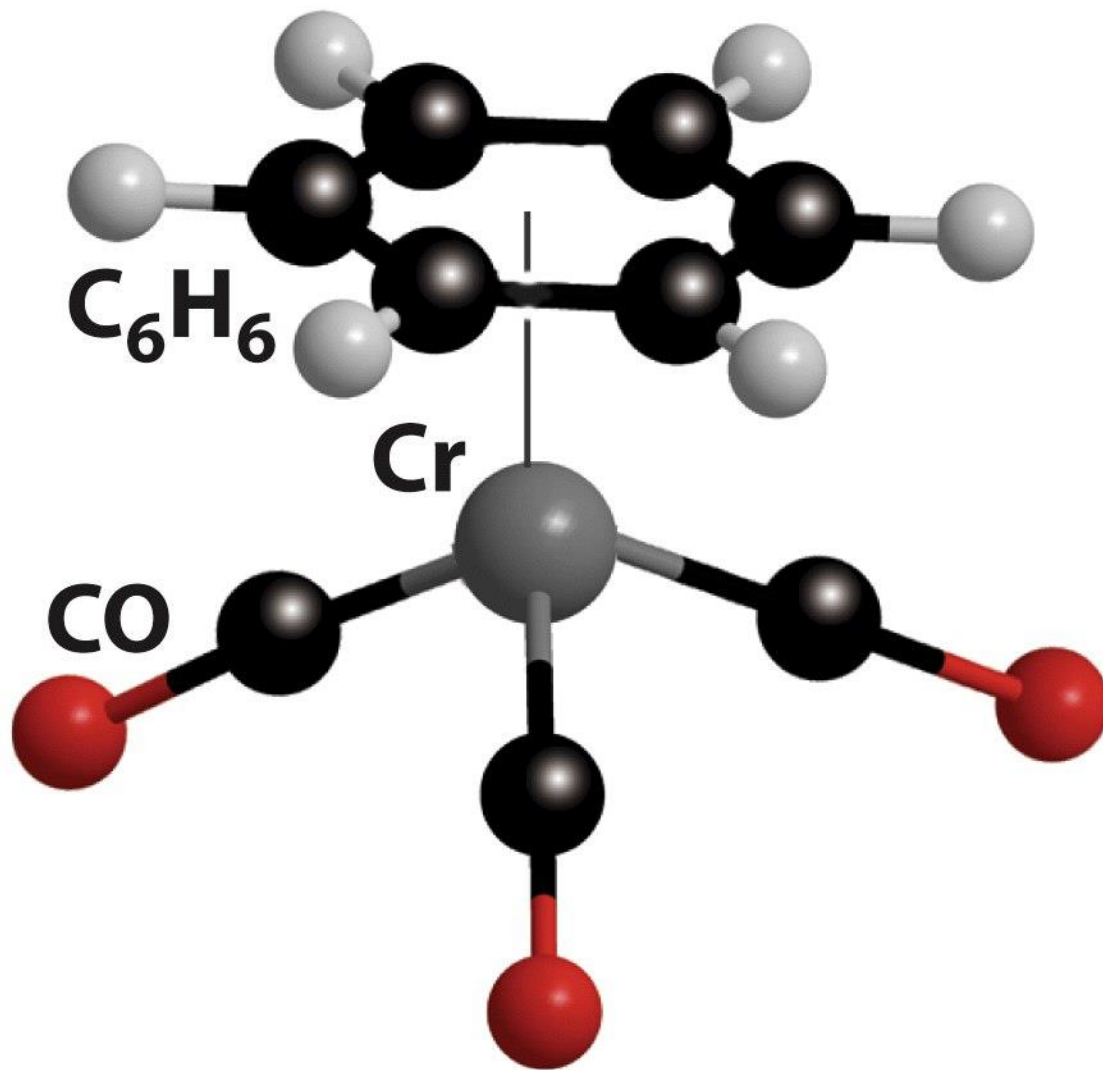
Half sandwich o *Piano stool*
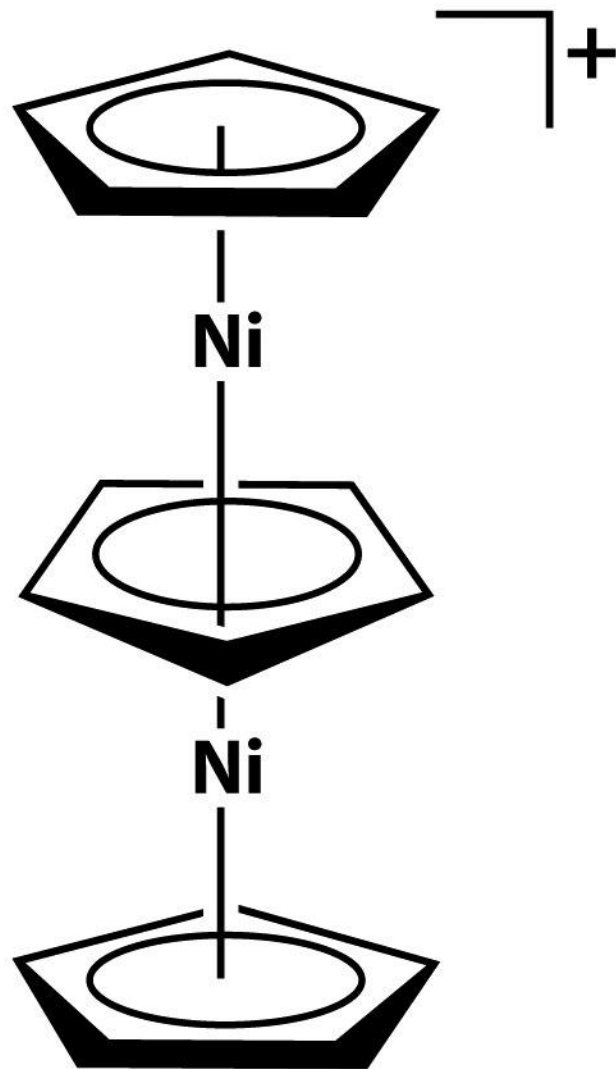
Triple decker o *doppio sandwich*
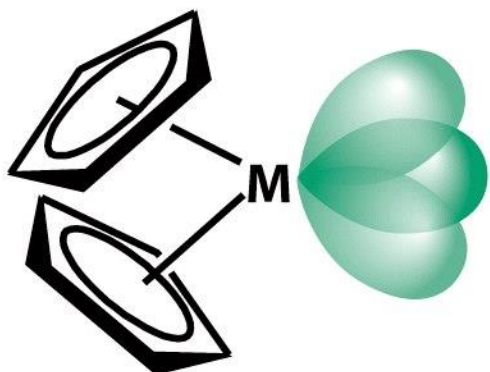
General form
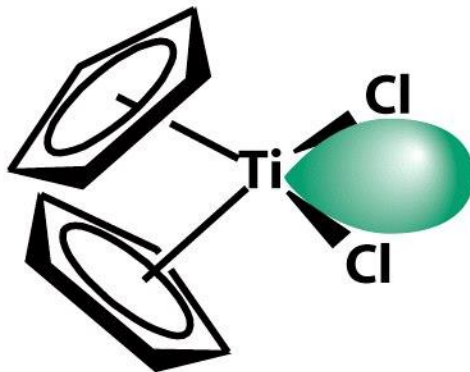
16-electron
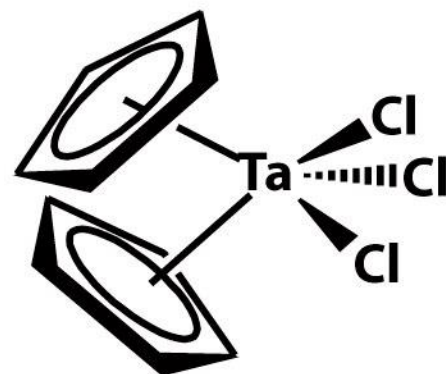
18-electron
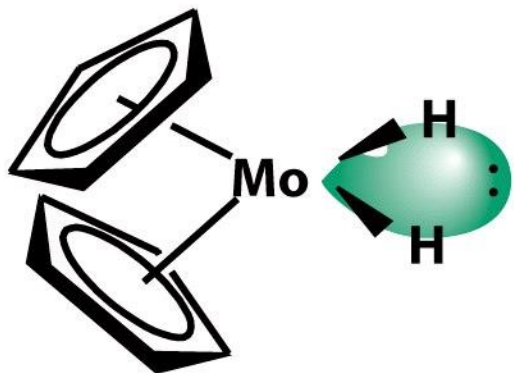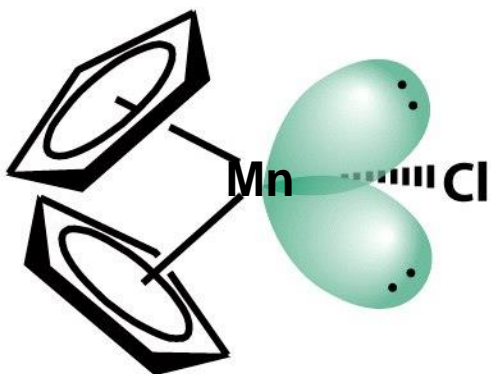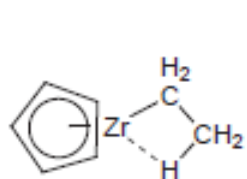
18-electron

18-electron

Diagramma di Walsh

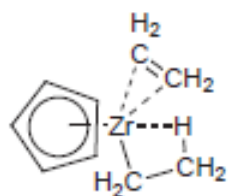*la geometria più stabile dipende sostanzialmente da quanti elettroni porta il metallo*

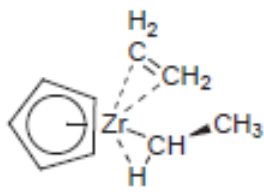HOMO
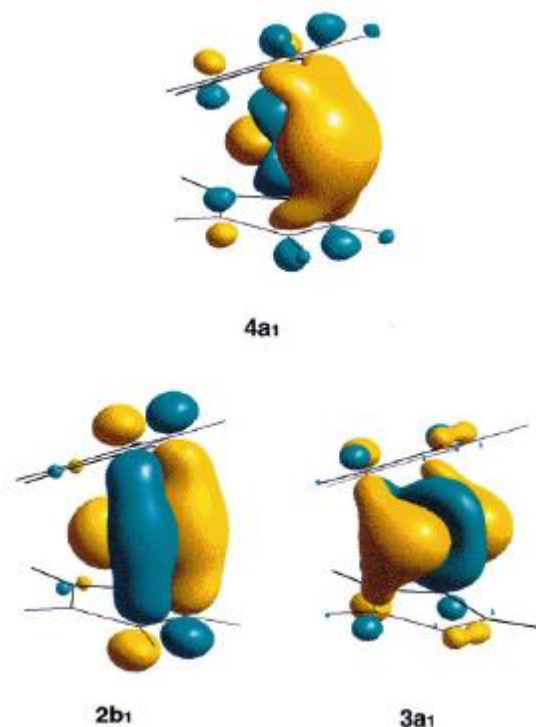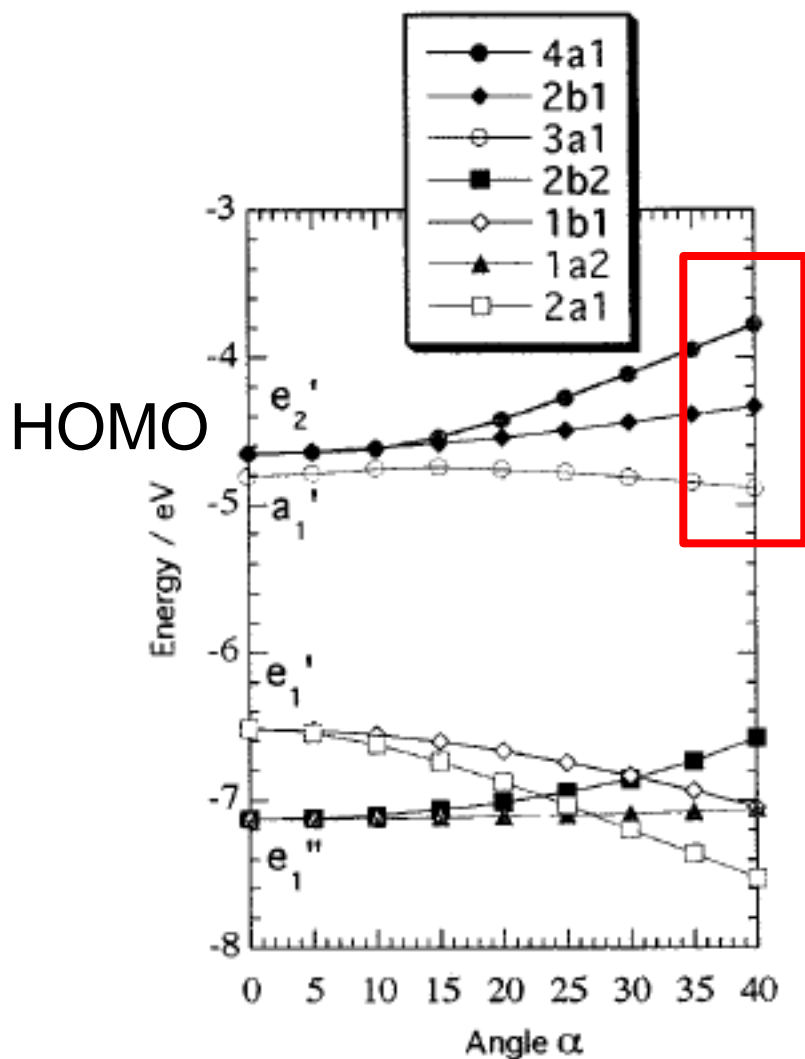
α è l'angolo fra i Cp; α = 0 corrisponde al ferrocene

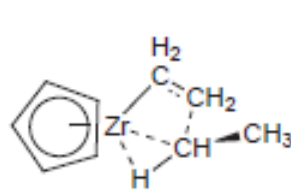# Cp$_2$ZrCl$_2$: catalizzatore tipo Ziegler-Natta per la polimerizzazione di olefine
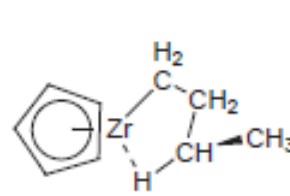

β-agostic resting state   β-agostic π-complex   α-agostic π-complex   α-agostic transition state   γ-agostic product   β-agostic resting state
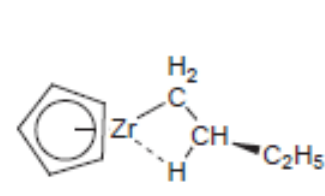
Elementi del blocco f

La	Ce	Pr	Nd	Pm	Sm	Eu	Gd	Tb	Dy	Ho	Er	Tm	Yb	Lu	Hf
Ac	Th	Pa	U	Np	Pu	Am	Cm	Bk	Cf	Es	Fm	Md	No	Lr	Rf

Lantanide generico = Ln, $4f^n5d^16s^2$

Attinide generico = An, $5f^n6d^17s^2$

Cp*

Sm

$Sm(\eta^5-Cp^*)_3$
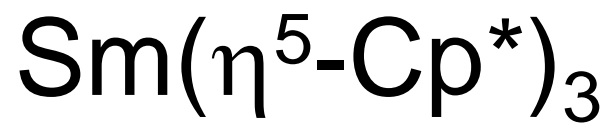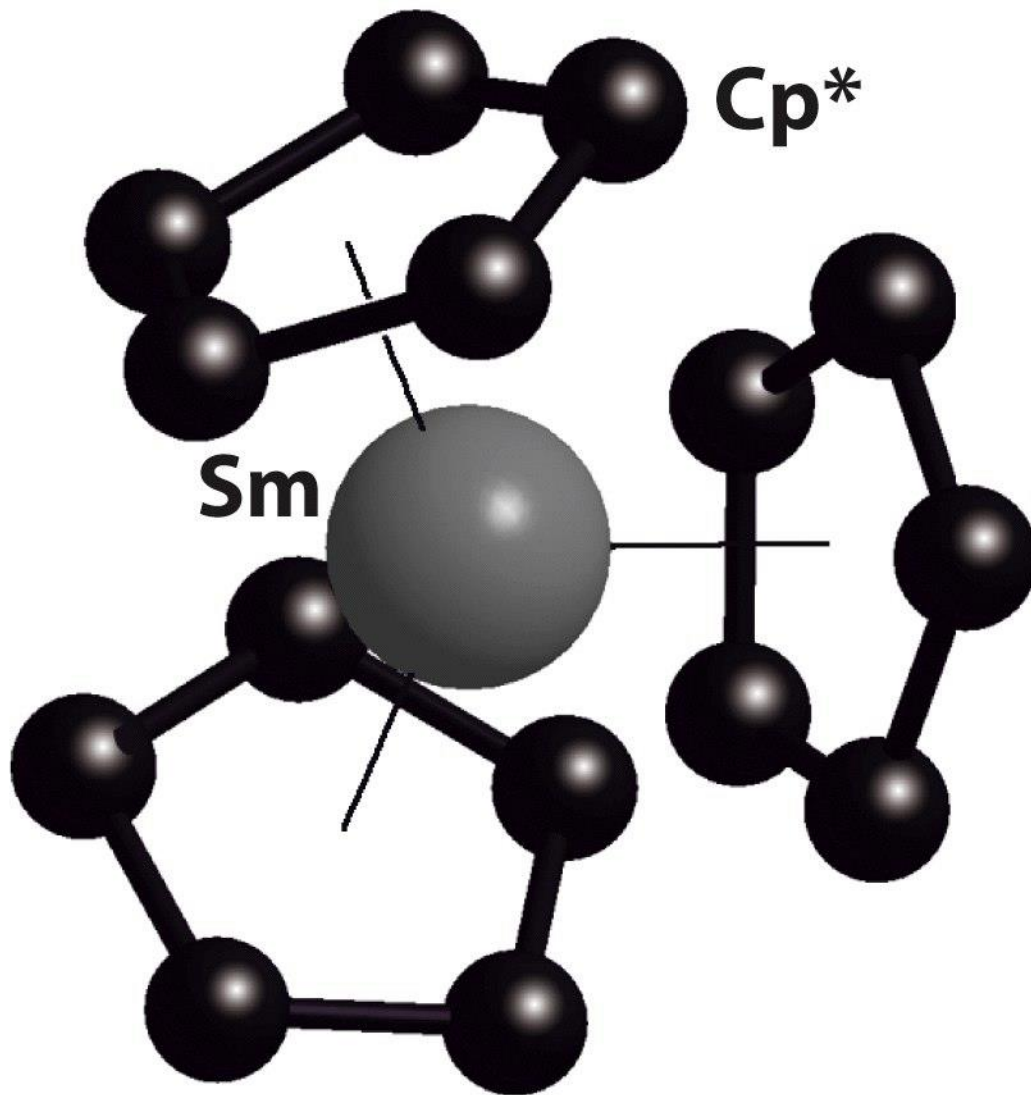
Synthesis and X-ray Crystal Structure of the First Tris(pentamethylcyclopentadienyl)–Metal Complex: (η^5-C$_5$Me$_5$)$_3$Sm

William J. Evans,* Shirley L. Gonzales, and Joseph W. Ziller
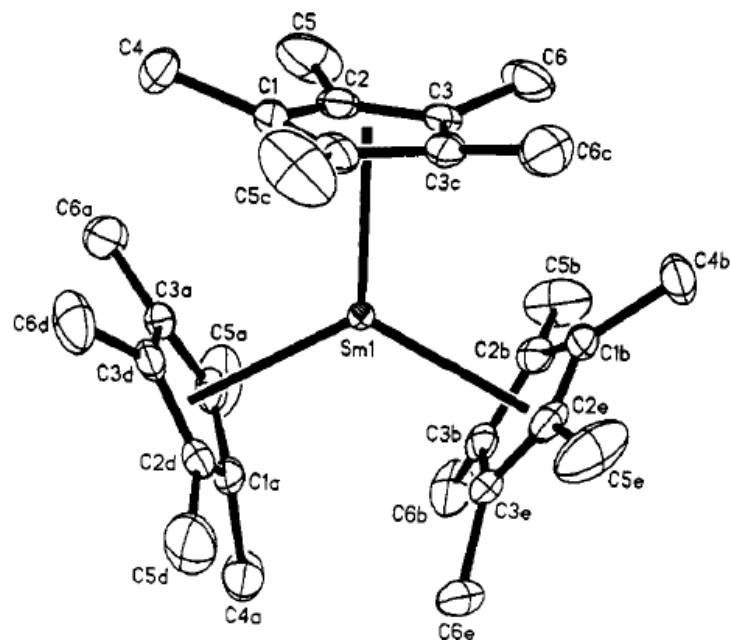
Figure 1. Molecular structure of (C$_5$Me$_5$)$_3$Sm (**2**) with probability ellipsoids drawn at the 50% level.
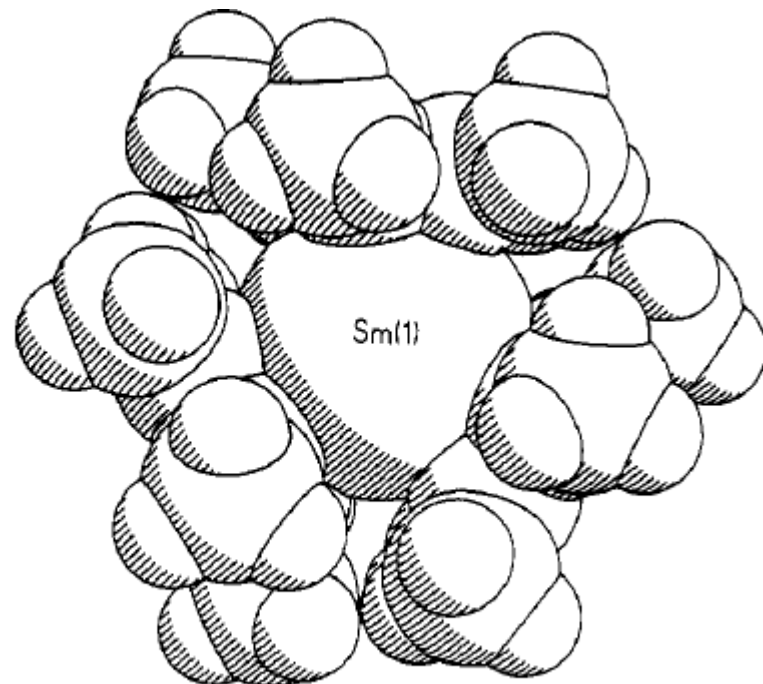
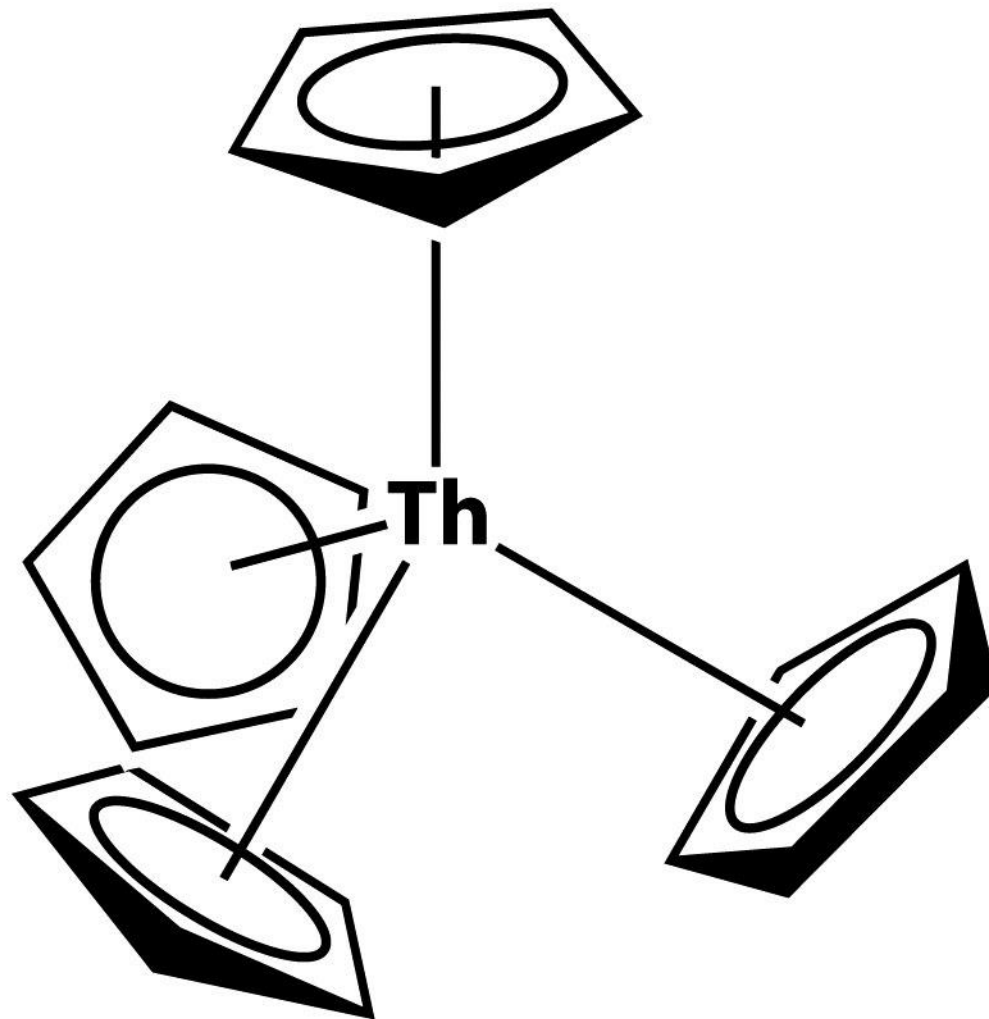**Figure 2.** Space-filling model of (C$_5$Me$_5$)$_3$Sm (**2**).

$$Sm(\eta^1\text{-}Cp^*)(\eta^5\text{-}Cp^*)_2$$

$$Sm(\eta^5\text{-}Cp^*)_3 \rightleftharpoons Sm(\eta^1\text{-}Cp^*)(\eta^5\text{-}Cp^*)_2$$

Th(Cp)$_4$

$U(Cp)_4$

U(Cp*)₃Cl

Torocene

Th

Th(C₈H₈)₂

$U(C_8H_8)_2$

Uranocene